Supporting Information

More Electrons on Fe and FeN_2 Promote Nitrogen Fixation Efficiency

Jin Feng[1], Xinlu Wang[1], Wenxing Xu[1], Xiaorui Xu[1], Dapeng Zhang[1]*,

1 Key Laboratory of Life-Organic Analysis of Shandong Province, School of Chemistry and Chemical Engineering, Qufu Normal University, P. R. China

*Corresponding author.
E-mail: zdp1014636837@hotmail.com

System	E_{bind}	E_{coh}	E_{clus}
Fe/g-C_3N_4	-7.26	-4.06	-3.20
Fe-Ce/g-C_3N_4	-6.97	-4.06	-2.92
Fe/Nv-g-C_3N_4	-8.26	-4.06	-4.21
Fe-Ce/Nv-g-C_3N_4	-8.00	-4.06	-3.94

Table S1. Cohesive energies (E_{coh}), binding energies (E_{bind}) and cluster energies (E_{clus}) for Fe in Fe/g-C_3N_4, Fe-Ce/g-C_3N_4, Fe/Nv-g-C_3N_4, Fe-Ce/Nv-g-C_3N_4. All energies are in eV.

	Fe/g-C_3N_4			Fe/Nv-g-C_3N_4			Fe-Ce/g-C_3N_4			Fe-Ce/Nv-g-C_3N_4		
	x	y	z	x	y	z	x	y	z	x	y	z
C	3.602	4.693	0.832	3.566	4.627	0.713	3.615	4.707	0.611	3.612	4.670	0.825
C	1.296	0.695	0.554	1.172	0.594	0.714	1.244	0.674	0.706	1.191	0.599	1.328
C	5.849	0.669	1.318	5.760	0.640	1.312	5.835	0.677	1.342	5.804	0.677	0.777
C	2.397	2.728	0.474	2.297	2.645	0.501	2.449	2.656	0.335	2.382	2.639	1.034
C	3.535	0.623	1.061	3.427	0.541	1.232	3.522	0.602	1.132	3.509	0.523	1.092
C	4.682	2.720	1.230	4.619	2.611	1.063	4.723	2.711	0.933	4.613	2.618	0.402
C	0.015	10.817	0.485	13.984	10.516	0.613	14.229	10.835	0.663	13.999	10.621	1.249
C	2.328	6.887	0.854	2.397	6.840	0.920	2.350	6.886	0.660	2.406	6.858	0.791
C	0.079	6.858	1.320	0.221	6.728	1.505	0.086	6.907	1.284	0.109	6.778	0.610
C	1.212	8.849	0.409	1.152	8.737	0.529	1.215	8.902	0.483	1.179	8.838	1.044
C	4.886	6.876	0.924	5.008	6.762	0.869	4.888	6.890	0.624	4.991	6.851	0.851
C	5.940	8.865	1.349	6.045	8.857	1.030	5.925	8.898	0.986	6.062	8.920	0.639
C	10.727	4.686	1.245	10.884	4.822	1.223	10.668	4.705	1.408	10.782	4.891	1.229
C	8.393	0.664	1.157	8.313	0.884	1.133	8.358	0.664	1.271	8.309	0.922	0.692
C	12.970	0.699	0.555	12.901	0.674	0.684	12.960	0.668	0.714	12.894	0.692	1.231
C	9.592	2.697	1.342	9.571	2.890	1.344	9.547	2.687	1.578	9.491	2.949	0.987
C	10.670	0.635	0.660	10.601	0.756	0.727	10.647	0.595	0.864	10.613	0.761	0.834
C	11.942	2.727	0.928	11.943	2.782	0.926	11.851	2.672	1.181	11.783	2.763	1.558
C	7.142	10.815	1.503	7.170	10.859	1.282	7.101	10.823	1.379	7.185	10.936	0.811
C	9.451	6.883	1.235	9.677	7.019	1.192	9.412	6.886	1.287	9.604	7.080	1.365
C	7.192	6.862	0.787	7.376	6.848	0.931	7.193	6.851	0.680	7.297	6.909	1.285
C	8.356	8.872	1.569	8.477	8.975	1.414	8.289	8.867	1.574	8.453	9.059	1.203
C	12.018	6.889	1.263	12.295	7.102	1.359	11.966	6.888	1.354	12.189	7.163	1.053
C	13.073	8.883	0.864	12.978	8.421	1.006	13.045	8.926	1.122	12.925	8.500	1.164
N	0.011	12.293	0.485	14.079	12.202	0.668	14.222	12.303	0.653	14.094	12.226	1.307
N	4.720	4.052	1.291	4.703	3.941	1.017	4.712	4.034	1.026	4.701	3.960	0.433
N	1.324	2.006	0.159	1.224	1.882	0.252	1.275	2.007	0.277	1.230	1.995	1.349
N	4.704	0.008	1.200	4.621	12.280	1.452	4.661	0.049	1.506	4.727	0.024	1.249
N	5.872	2.055	1.420	5.791	1.991	1.177	5.876	2.056	1.217	5.775	1.989	0.420
N	2.341	0.004	1.002	2.239	12.258	1.223	2.308	0.047	1.212	2.365	12.292	1.437
N	2.511	4.074	0.348	2.424	3.994	0.346	2.455	4.013	0.245	2.516	3.966	1.294
N	3.538	2.034	0.969	3.447	1.946	0.978	3.614	1.949	0.551	3.403	1.899	0.399

N	1.143	10.160	0.121	0.952	10.037	0.251	1.102	10.197	0.219	1.023	10.140	1.165
N	1.285	6.263	1.432	1.478	6.172	1.590	1.242	6.206	1.174	1.296	6.100	0.479
N	2.332	8.101	0.282	2.306	8.058	0.339	2.279	8.138	0.203	2.360	8.161	1.075
N	0.049	8.190	0.869	0.080	8.020	1.049	0.085	8.257	1.158	0.014	8.081	0.892
N	3.618	6.141	0.855	3.710	6.068	0.791	3.607	6.144	0.596	3.681	6.125	0.841
N	4.810	8.134	1.368	4.943	8.098	0.946	4.794	8.189	0.906	4.968	8.138	0.497
N	6.023	6.240	0.538	6.234	6.082	0.839	6.043	6.218	0.372	6.148	6.159	1.203
N	5.961	10.186	1.472	6.043	10.199	0.980	5.957	10.226	1.019	6.084	10.240	0.415
N	7.130	12.281	1.338	7.074	0.032	1.283	7.097	12.287	1.360	7.106	0.078	0.761
N	11.872	4.072	0.928	11.972	4.139	0.879	11.833	4.017	1.099	11.868	4.121	1.642
N	8.401	2.027	1.434	8.341	2.264	1.414	8.367	2.023	1.587	8.296	2.326	0.800
N	11.828	0.043	0.324	11.702	0.055	0.491	11.798	0.047	0.483	11.784	0.126	0.757
N	13.060	2.025	0.837	13.021	2.015	0.879	13.009	2.029	0.984	12.933	2.053	1.575
N	9.475	0.026	0.707	9.367	0.204	0.729	9.443	0.036	0.802	9.459	0.263	0.462
N	9.564	4.021	1.553	9.703	4.199	1.586	9.521	4.021	1.664	9.665	4.257	0.794
N	10.721	2.014	1.021	10.688	2.140	1.012	10.713	1.945	1.441	10.577	2.116	1.441
N	8.324	10.201	1.733	8.348	10.299	1.603	8.223	10.183	1.800	8.337	10.389	1.230
N	8.390	6.248	0.681	8.572	6.293	0.832	8.394	6.237	0.674	8.465	6.340	1.553
N	9.457	8.118	1.748	9.656	8.337	1.486	9.378	8.111	1.821	9.632	8.424	1.277
N	7.169	8.201	1.181	7.295	8.220	1.145	7.150	8.203	1.047	7.259	8.287	1.059
N	10.730	6.137	1.276	10.930	6.346	1.245	10.706	6.138	1.380	10.846	6.395	1.261
N	11.935	8.172	0.899	13.267	6.211	1.727	11.923	8.204	1.171	13.145	6.213	0.676
N	13.152	6.253	1.624	12.874	9.850	0.905	13.179	6.200	1.468	12.852	9.910	1.337
N	13.107	10.216	0.823	□-	-	-	13.082	10.242	1.033	□-	□-	□-
Fe	7.152	3.309	1.540	6.825	3.917	1.150	7.130	3.312	1.447	6.812	3.848	0.813
Ce	-	-	-	-	-	-	0.048	4.102	0.808	0.059	4.115	1.465

Table S2 The optimized coordinates for the structures in Fig. 1a-d.

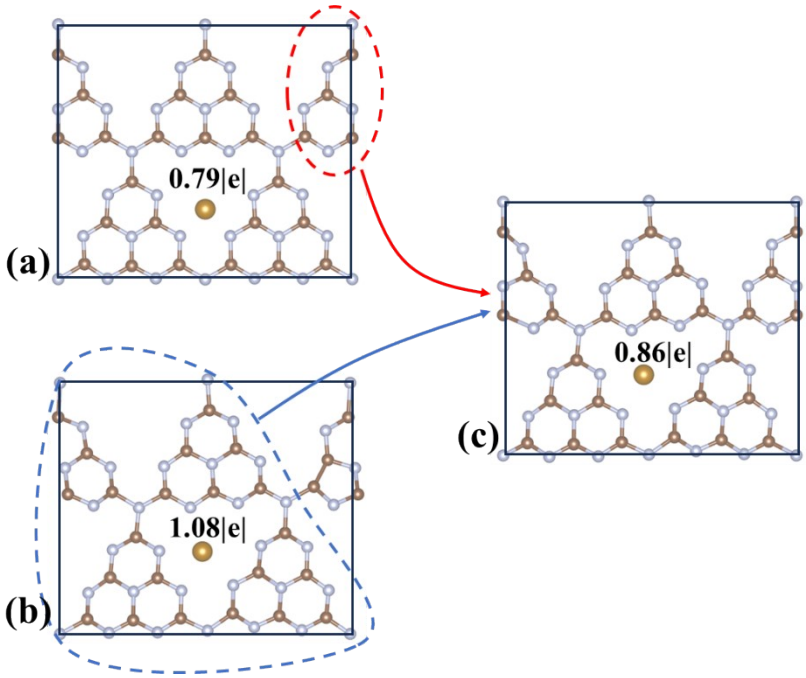

Fig. S1 (a) Structure of Fe/g-C_3N_4, consistent with Figure 1a. (b) Fe/Nv-g-C_3N_4, consistent with Figure 1b. (c) The structure of Fe/g-C_3N_4, consisting of the red part in (a) and the blue part in (b).

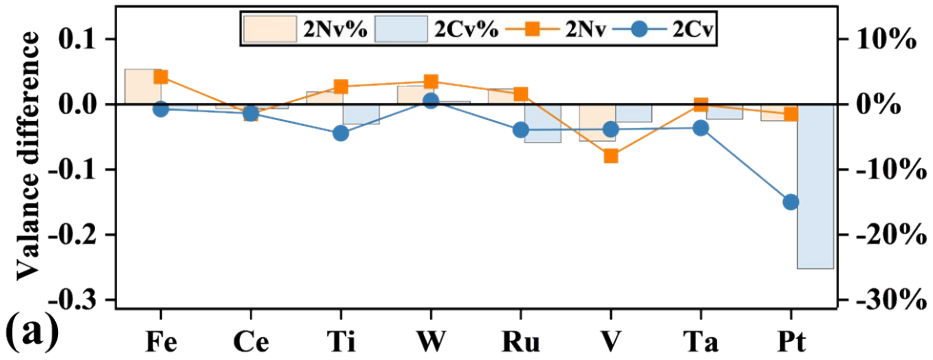

Fig. S2 (a) The valance difference for element X between double defected and pristine g-C_3N_4

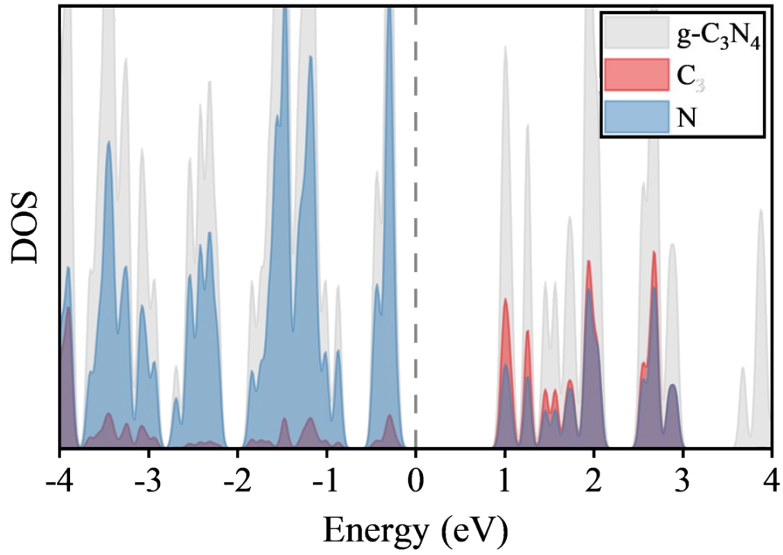

Fig. S3 The DOS of g-C_3N_4

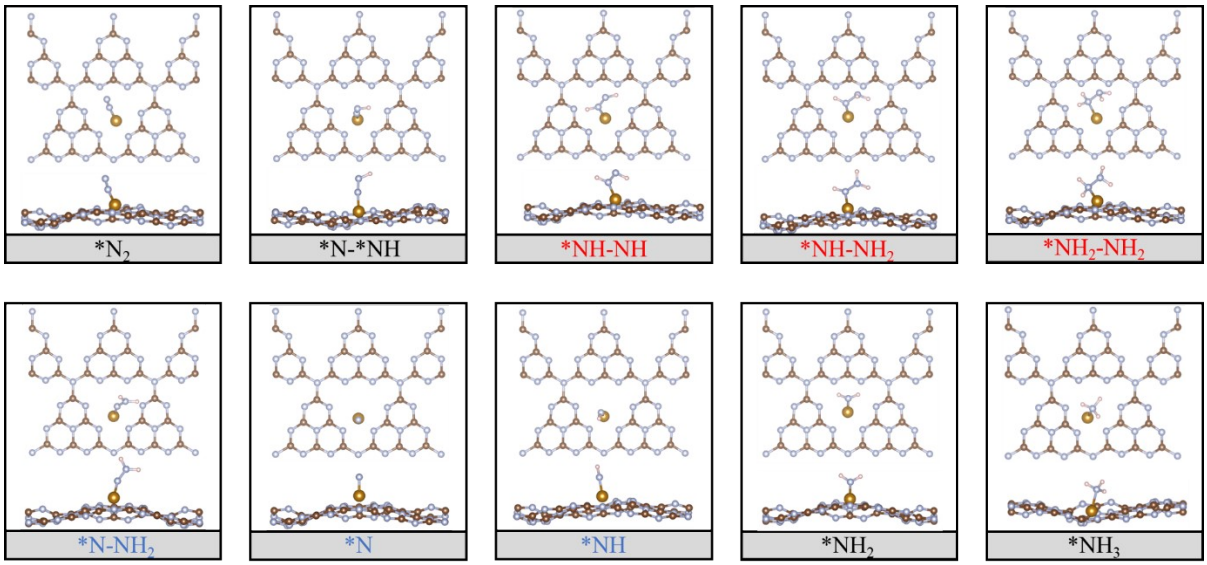

Fig. S4 Structures of the reaction intermediates for N_2 reduction on Fe/g-C_3N_4 through the distal (blue) and alternating (red) pathway.

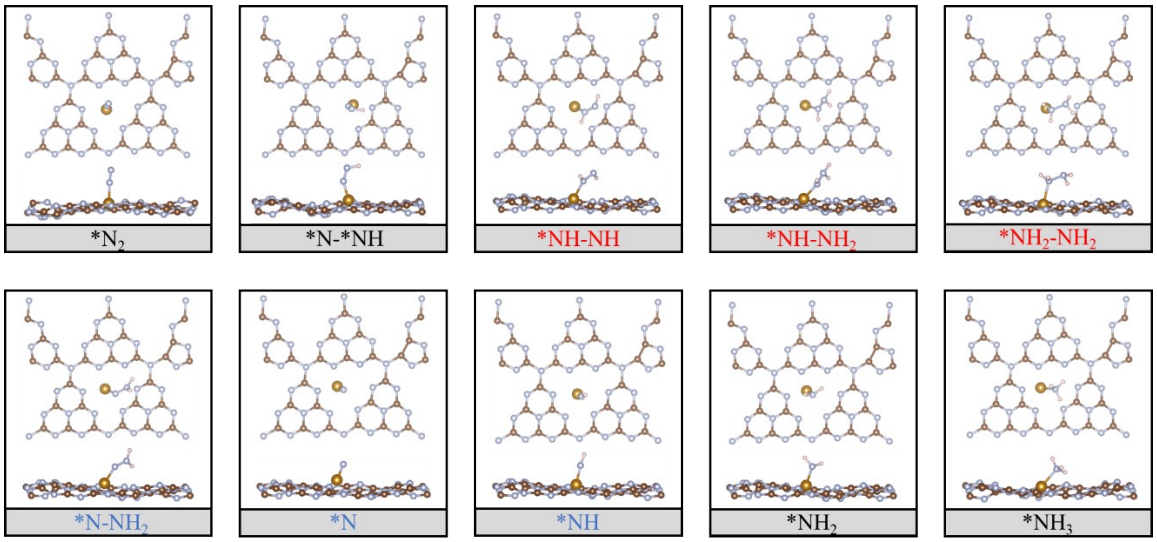

Fig. S5 Structures of the reaction intermediates for N_2 reduction on Fe/Nv-g-C_3N_4 through the distal (blue) and alternating (red) pathway.

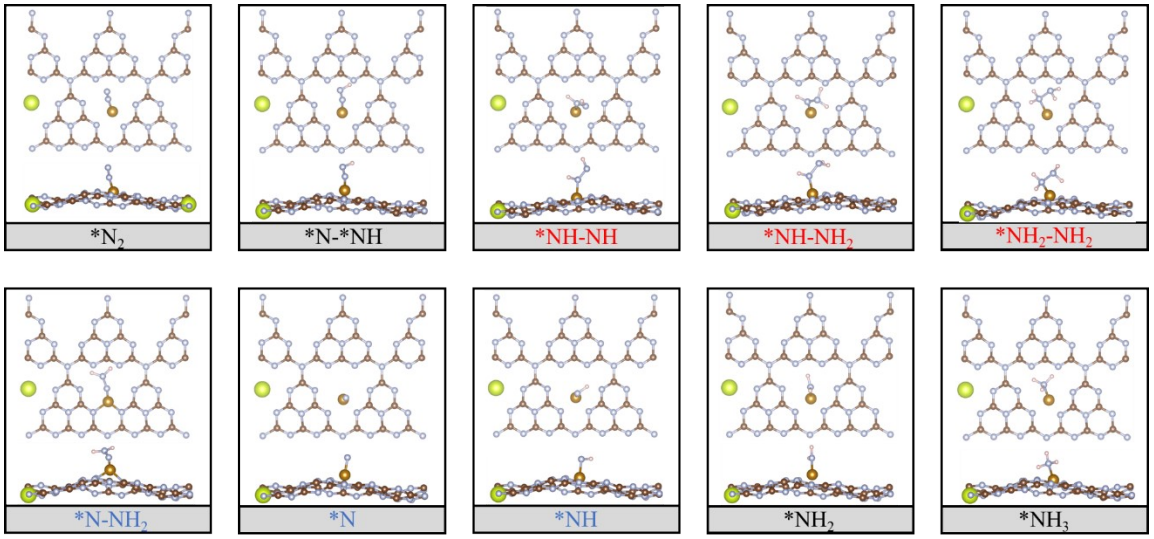

Fig. S6 Structures of the reaction intermediates for N_2 reduction on Fe-Ce/g-C_3N_4 through the distal (blue) and alternating (red) pathway.

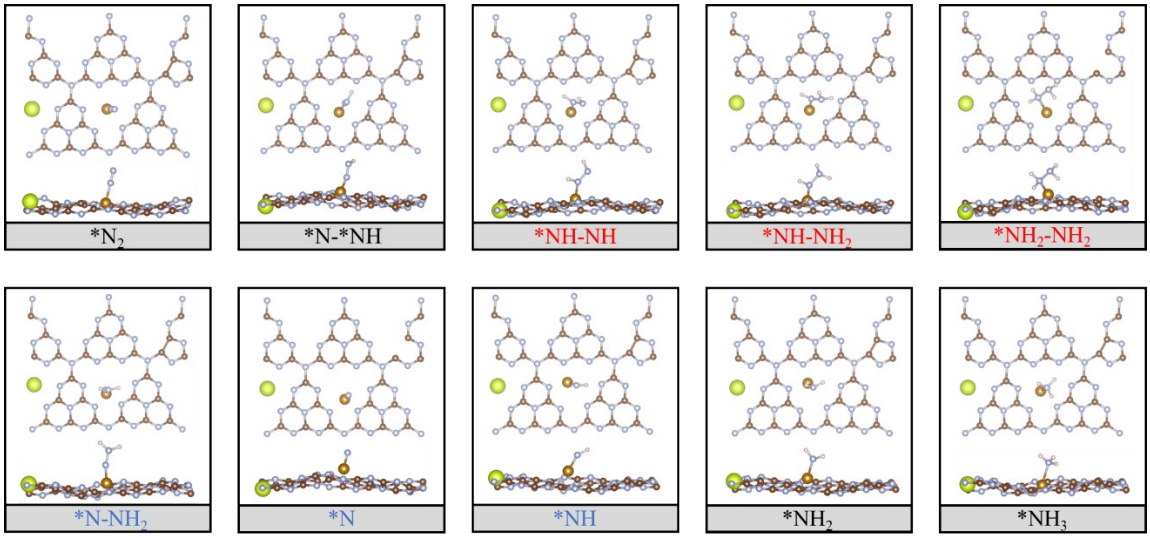

Fig. S7 Structures of the reaction intermediates for N_2 reduction on Fe-Ce/Nv-g-C_3N_4 through the distal (blue) and alternating (red) pathway.

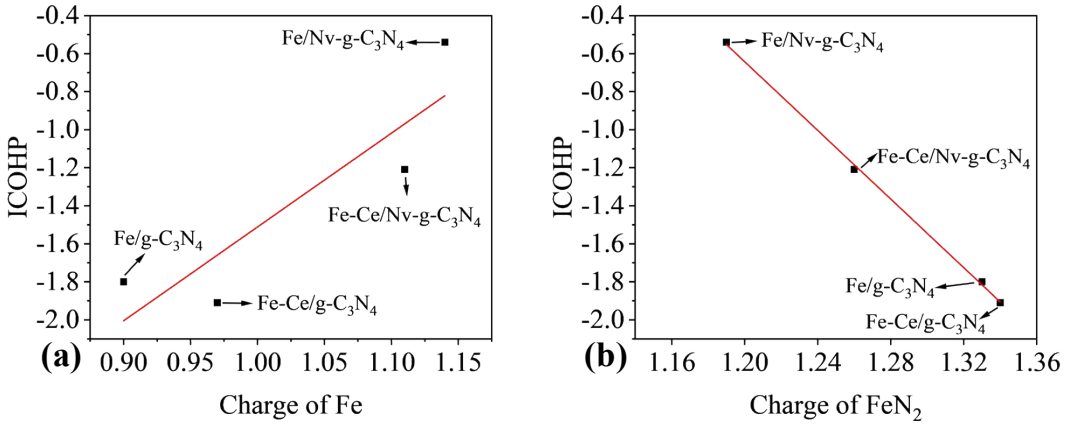

Fig. S8 Linear relationship between ICOHP and charge of Fe (a) and FeN_2 (b).

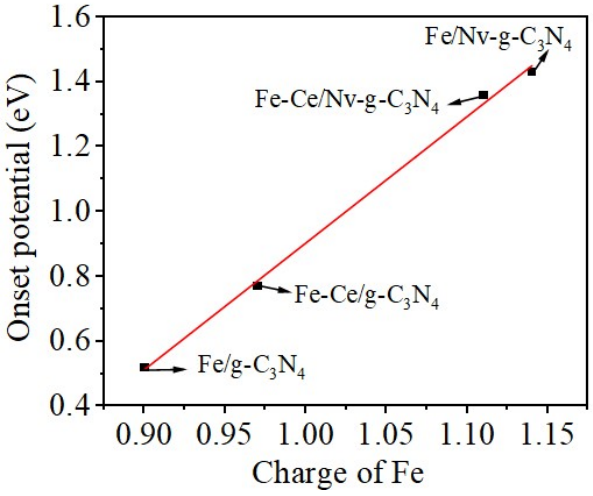

Fig. S9 Linear relationship between onset potential and charge of Fe.

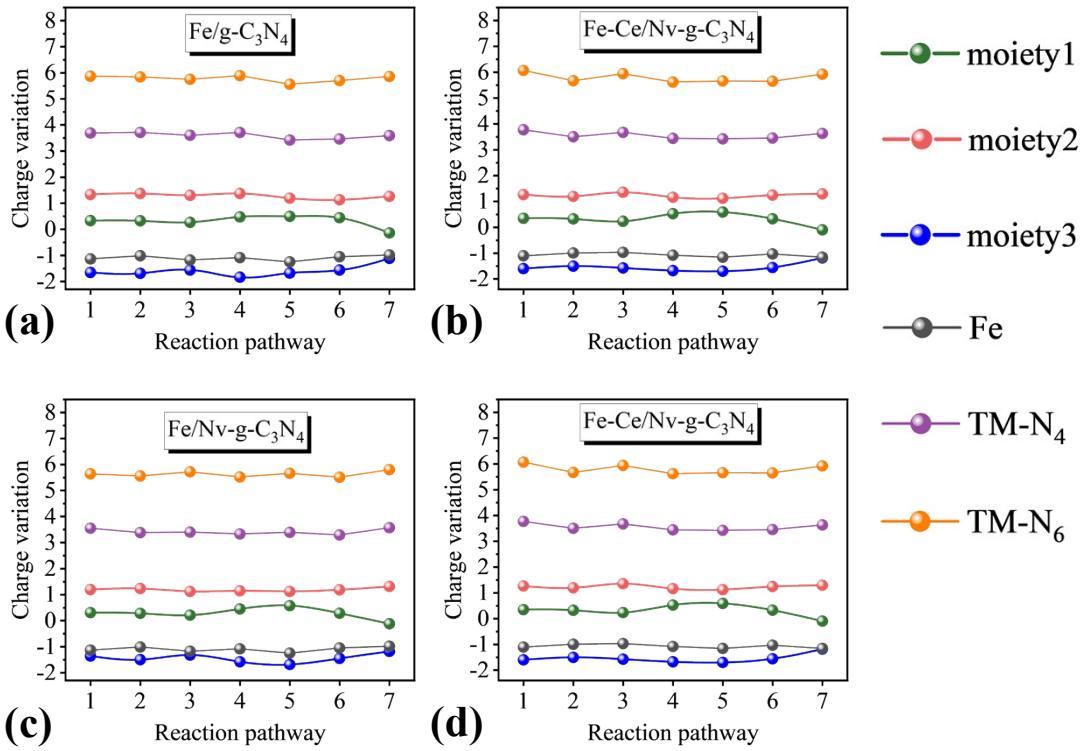

Fig. S10 Charge variation of the six moieties for (a) Fe/g-C_3N_4, (b) Fe-Ce/g-C_3N_4 (c)Fe/Nv-g-C_3N_4 and (d) Fe-Ce/Nv-g-C_3N_4. Moieties 1, 2, 3, Fe, TM-N_4 and TM-N_6 denote adsorbed N_xH_y, TM-N_2 composed of TM and two N atom beside it, and g-C_3N_4, isolated Fe atom, TM-N_4 composed of TM and four N atom beside it, TM-N_6 composed of TM and six N atom beside it respectively.

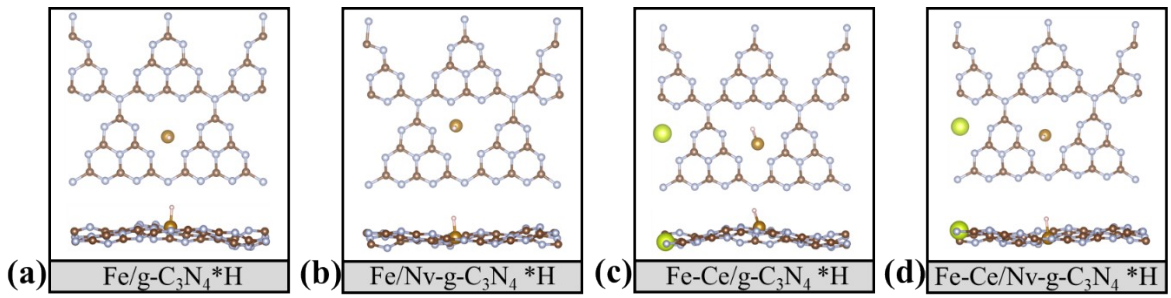

Fig. S11 H is adsorbed in the top and side views of the structures of (a) Fe/g-C_3N_4, (b)Fe/Nv-g-C_3N_4, (c) Fe-Ce/g-C_3N_4 and (d) Fe-Ce/Nv-g-C_3N_4.